



DISCUSSION PAPER PI-2502

Incorporating Vitagions into Stochastic Longevity Models.

Maria Carannante, Valeria D'Amato, Cinzia De Palo and Maria Sole Staffa

October 2025

ISSN 1367-580X

The Pensions Institute
Bayes Business School
City, University of London
106 Bunhill Row
London EC1Y 8TZ
UNITED KINGDOM
<http://www.pensions-institute.org/>

Incorporating Vitagions into Stochastic Longevity Models

Maria Carannante, European University of Rome,

`maria.carannante@unier.it`

Valeria D’Amato, Sapienza Università di Roma,

`valeria.damato@uniroma1.it`

Cinzia Di Palo, Università di Cassino e del Lazio Meridionale,

European University of Technology EUt+, European Union

`c.dipalo@unicas.it`

Maria Sole Staffa, European University of Rome,

`mariasole.staffa@unier.it`

October 27, 2025

Abstract

Assessing mortality dynamics remains a central challenge in demographic, actuarial, and public health research, primarily due to the difficulty of producing reliable forecasts. This complexity is particularly highlighted during periods with large deviations from long-term trends, such as sudden mortality increases due to pandemics or decreases driven by medical and technological breakthroughs.

In this context, we address the need for enhanced stochastic models that integrate sudden and significant mortality improvements, termed “vitagions”, into forward-looking forecasts. While foundational stochastic mortality models, such as those developed by Cairns et al. (2006b,a, 2009), provide a robust basis, they do not explicitly account for exogenous, forward-looking innovations. Building on this literature, we incorporate vitagions, defined as stochastic agents of mortality improvement associated with biomedical innovation and other external shocks (Woo (2014); Carannante et al. (2024)). Vitagions capture health-related advances, from disease prevention to advanced therapies, that can trigger persistent and one-sided mortality reductions.

This paper makes one main contribution. We extend the Lee–Carter (LC) and Cairns–Blake–Dowd M6 (CBD M6) models by adding an exogenous innovation covariate that captures age-specific sensitivity to a detrended indicator of pharmaceutical innovation (constructed from FDA/EMA approvals), and we address identifiability through explicit normalisations and orthogonality constraints. An empirical analysis employs data from the U.S., France, and Italy, which show different historical mortality patterns. Scenario-based simulations deliver clearer period dynamics while preserving baseline age profiles.

Keywords: stochastic mortality models; vitagions; longevity risk; Lee–Carter; Cairns–Blake–Dowd; medical innovation.

1 Introduction

Mortality modelling underpins risk measurement for life insurers and pension systems. While stochastic models such as Lee and Carter (1992) and the CMI/CBD family (e.g. Cairns et al., 2009; Haberman and Renshaw, 2011) capture broad time and age effects, they typically omit explicit relationships between innovation in medical therapies and mortality improvements. We contribute by incorporating an exogenous indicator of medical innovation into the Lee–Carter and the Cairns–Blake–Dowd (variant M6) models, addressing identifiability and documenting the empirical relevance across the US and other selected EU countries. Using data for the United States, France, and Italy, we report empirical gains in fit and interpretability and conduct scenario-based simulations to assess robustness under alternative vitagion assumptions.

1.1 Related Literature

We position our study in the framework of mortality modelling with exogenous drivers and health innovation, see also Niu and Melenberg (2014) for links between mortality and macro trends.

2 Models with Medical Innovation

This Section explores some stochastic models to incorporate the mortality improvements driven by vitagions. Indeed, traditional extrapolative models, such as the Lee-Carter (LC) model, either discrete- or continuous-time approaches, predict future mortality relying exclusively on historical data, without integrating external projections or assumptions about future developments. They “...do not attempt to incorporate assumptions about advances in medical science or specific environmental changes: no information other than previous history is taken into account...”, Pitacco (2009), since they implicitly assume that all relevant information about future mortality trends is encapsulated within the historical observations of death rates. Hence, while effective in many contexts, they may overlook unexpected medical advancements or healthy lifestyle changes.

2.1 The Lee-Carter model with medical improvements

The Lee-Carter model, widely used for mortality projections, models the mortality rate at age x in the future calendar year t as a stochastic process denoted by $m(x, t)$. The basic equation for the Lee-Carter model is as follows.

$$\log m(x, t) = \alpha(x) + \beta(x) \kappa(t) + \theta(x) I(t) + \varepsilon(x, t), \quad (1)$$

where $\alpha(x)$ is the average level of mortality by age; $\beta(x)$ measures the sensitivity of age to temporal changes in mortality; $\kappa(t)$ is the temporal trend of mortality; $\theta(x)$ captures the

age-specific sensitivity to pharmaceutical innovation; and $I(t)$ is the time series of detrended proportion of new medical entities (NMEs) introduced in year t .

Introducing the time-varying covariate into the LC model raises a nontrivial identifiability problem rooted in the temporal relation between the period factor, $\kappa(t)$, and the covariate, $I(t)$. Because predictions are unchanged by reallocating effects, the period factor and the covariate are not separately identifiable without extra restrictions. Accordingly, beyond the standard LC normalisations $\sum_x \beta(x) = 1$ and $\sum_t \kappa(t) = 0$, to ensure identifiability in the presence of the covariate, we impose:

$$\text{cov}(\kappa(t), I(t)) = 0, \quad \boldsymbol{\kappa} = (\kappa(1), \dots, \kappa(T)) \neq \mathbf{0}.$$

The temporal relation between $\kappa(t)$ and $I(t)$ can be estimated via a time-series regression.

2.2 The CBD-M6 with medical innovation

Among the most influential contributions to the mortality-modelling literature, Cairns et al. (2009) proposed seven stochastic specifications that have become standard in actuarial literature and practice due to their flexibility and empirical performance. Conceptually, our approach is related to the CBD-M6 specification, see Hunt and Blake (2014), who outline a general procedure for constructing single-population mortality models by combining parametric components with expert judgment. We extend this perspective by explicitly incorporating medical and pharmaceutical innovation via vitagions, thereby moving beyond the transitory shocks typically modelled in the existing literature.

The CBD M6 model, proposed by Cairns et al. (2009), is specified as

$$\text{logit } m(t, x) = \kappa_1(t) + \kappa_2(t)(x - \bar{x}) + \gamma(t - x), \quad (2)$$

where x is the age, $\bar{x} = \frac{1}{n} \sum_{i=1}^n x_i$ is the average age in the population, $\kappa_1(t)$ and $\kappa_2(t)$ capture, respectively, the overall temporal trend of mortality and the temporal trend of

mortality as discrepancy with respect to $(x - \bar{x})$, and $\gamma(t - x)$ is the cohort effect.

One imposes the following restrictions on the cohort effect to ensure parameter uniqueness in the basic M6 model.

$$\sum_c \gamma(c) = 0, \quad \sum_c c \gamma(c) = 0, \quad (3)$$

where $c = t - x$. These conditions eliminate non-identifiability due to arbitrary shifts of the cohort component.

To include the exogenous driver $I(t)$, in our application, the indicator of pharmaceutical improvements, but the considerations apply to any covariate, we introduce in equation (2) an additional term $\theta(x)I(t)$, where $\theta(x)$ is the age-specific sensitivity of the log-odds mortality to the effect of the covariate.

The extended CBD M6 model specification is

$$\text{logit } m(t, x) = \kappa_1(t) + \kappa_2(t)(x - \bar{x}) + \gamma(t - x) + \theta(x)I(t). \quad (4)$$

As is well-known from the LC model, see Niu and Melenberg (2014), adding the exogenous variable, $I(t)$, creates an identifiability problem between the time-trend, $\kappa_1(t)$, and the age-specific term, $\theta(x)$. In particular, for any constant $e \in \mathbb{R}$, the transformation

$$\tilde{\kappa}_1(t) = \kappa_1(t) + eI(t), \quad \tilde{\theta}(x) = \theta(x) - e \quad (5)$$

leaves the model fitting unchanged, since

$$\tilde{\kappa}_1(t) + \tilde{\theta}(x)I(t) = (\kappa_1(t) + eI(t)) + (\theta(x) - e)I(t) = \kappa_1(t) + \theta(x)I(t). \quad (6)$$

This shows that different pairs $(\kappa_1(t), \theta(x))$ produce the same prediction, making $\kappa_1(t)$ and $\theta(x)$ not uniquely identifiable without additional restrictions.

Then, to ensure parameter identifiability in the extended CBD M6 model, we impose the

following restrictions

$$\sum_t I(t) = 0, \quad (7)$$

$$\text{cov}(\kappa_1(t), I(t)) = 0, \quad (8)$$

$$\sum_x \theta(x) = 1. \quad (9)$$

The first and second conditions are related to the stationarity of $I(t)$ and the absence of correlation between κ_1 and $I(t)$. In particular, these two constraints follow the estimation of an Ordinary Least Squares (OLS) model that captures the effect of $I(t)$ on κ_1 . This way, obtaining consistent estimators and managing the temporal and exogenous effects separately is possible.

The third restriction is essential for parameter identification. In the CBD M6 specification, the age sensitivity to the general trend of mortality is fixed, i.e. $\beta(x) = 1$ for all ages; hence, the effect of age cannot be absorbed in the relationship between $\kappa_1(t)$ and $I(t)$. In this case, the exogenous effect would shift the mean of $\theta(x)$ across all ages without distinguishing age-specific sensitivities. Therefore, the restriction $\sum_x \theta(x) = 1$ is required for model identifiability. More generally, the product $\theta(x)I(t)$ is invariant if $\theta(x)$ is multiplied by a constant c and $I(t)$ is divided by the same constant:

$$\tilde{\theta}(x)\tilde{I}(t) = (c\theta(x))\left(\frac{I(t)}{c}\right) = \theta(x)I(t). \quad (10)$$

A normalisation of $\theta(x)$ removes this scale indeterminacy and permits a clear interpretation of the exogenous covariate's effect on different ages.

3 The Medical Innovation Indicator

Let i denote the index in therapeutic classes, with $i \in \{1, \dots, p\}$. Denote by $n_i(t) \in \mathbb{N}_0$ the number of items of type i approved in year t and by

$$N_i = \sum_t n_i(t)$$

the total number of approvals of type i over the full time horizon. We define the type-specific indicator of innovation in medical therapies, say $I_i(t)$, as the proportion of therapies approved in year t on the total approved during the time horizon, that is

$$I_i(t) = \frac{n_i(t)}{N_i}, \tag{11}$$

so that $\sum_t I_i(t) = 1$ whenever $N_i > 0$. If $N_i = 0$ for some i , then we set $I_i(t) = 0$.

By construction, $I_i(t)$ measures the share of all approvals of type i that occur in year t ; hence, $I(t)$ summarises these shares across types according to economically or clinically meaningful weights.

4 Numerical Illustrations

4.1 Data sources

We present numerical illustrations for mortality rate trends under baseline and innovation-adjusted models, and discuss the impact of advanced therapies on mortality. We focus on the United States, France, and Italy because they combine deep, well-established health-care systems with a steady flow of new therapies, offer clear and frequent regulatory data, and provide long and reliable mortality series that line up over time, including through the COVID-19 shock.

Medical innovation. For the U.S., we rely on three official Food and Drug Administration (FDA) sources, see U.S. Food and Drug Administration (2025c,b,a):

- the **Purple Book Database of Licensed Biological Products**, which lists all approved biological products, available at: <https://purplebooksearch.fda.gov/>.
- the **Compilation of CDER NME and New Biologic Approvals (1985–2024)**, which lists new molecular entities (NMEs) and new biologics, and is a primary source for monitoring pharmaceutical innovation, available at: <https://www.fda.gov/drugs/drug-approvals-and-databases/compilation-cder-new-molecular-entity-nme-drug-and-new-biologic-approvals>
- the **Approved Cellular and Gene Therapy Products**, which lists the FDA-approved cell and gene therapy products, including the type of therapy, approval date, and regulatory status, available at: <https://www.fda.gov/vaccines-blood-biologics/cellular-gene-therapy-products/approved-cellular-and-gene-therapy-products>.

For the European Union, we use the EMA’s European Public Assessment Reports (EPAR), the official repository of centrally authorised medicinal products with detailed regulatory and clinical information, European Medicines Agency (2025). The downloadable datasets are available at <https://www.ema.europa.eu/en/medicines/download-medicine-data>.

Mortality. Mortality inputs—central death rates and exposures—are taken from the Human Mortality Database (Human Mortality Database, 2025). We use annual data for the United States from 1985 to 2023, and, for the European Union, we focus on France and Italy with comparable series spanning 1995–2023.

4.2 Numerical Estimation and Results

To capture forecast uncertainty, we simulate 50,000 paths of central rates of mortality m_x , based on ARIMA models. In particular, following the literature (Lee and Carter (1992);

Cairns et al. (2009); Haberman and Renshaw (2011)), we estimate a random walk with drift for $\kappa(t)$ and $I(t)$, and a first-order autoregressive model for $\gamma(t - x)$. Forecast projections are obtained from the log-normal white noise process across the 50,000 simulations.

United States Medical Innovation. We summarise FDA approvals with the weighted average of the component series $I_i(t)$ for $i \in \{\text{NDA}, \text{BLA}, \text{ATMP}\}$, where NDA is the acronym for New Drug Applications and denotes small-molecule, BLA stands for Biologics License Applications and covers biologics, and ATMP for Advanced Therapies and capture cell and gene therapies.

We plot the three component series that evolve differently; see Figure 1.

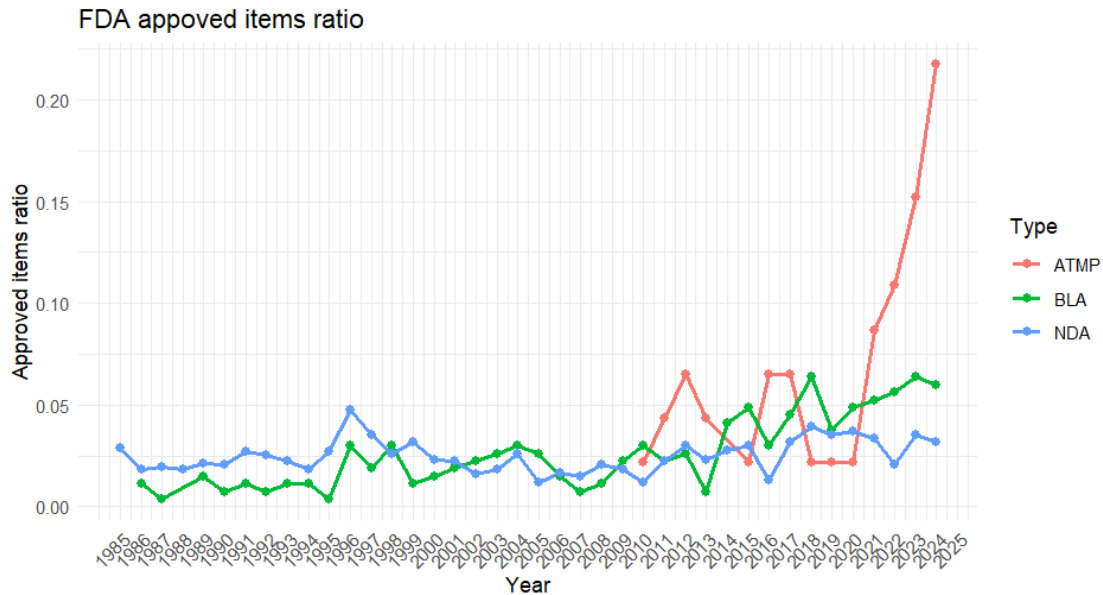


Figure 1: FDA-approved items, 1985–2024. Annual shares of approvals by type (NDA, BLA, ATMP).

NDA show a relatively stable flow over time, with values typically in the 0.02–0.05 range, consistent with a steady pace of small-molecule approvals. Biologics BLAs have risen progressively from the early 2000s and, in recent years, have surpassed NDAs, reflecting their growing role in therapeutic practice. Advanced therapies (ATMPs) were virtually absent before 2010, increased sharply from around 2015, and accelerate further after 2020; by 2025,

their share exceeds 0.2, signalling the rapid expansion of cell and gene therapies.

These dynamics suggest three broad phases: a pre-2000 period dominated by NDAs, with few biologics and no ATMPs, a 2000-2015 transition as biologics gain traction, and a post-2015 regime shift in which ATMPs expand at an exceptional pace and begin to rival and surpass the other categories.

Europe Medical Innovation. We summarise EMA approvals with the weighted average of the component series $I_i(t)$ for $i \in \{\text{NME}, \text{ATMP}\}$, where NMEs represent traditional therapies and ATMPs represent advanced therapies, see Figure 2.

NME approvals display a generally linear, increasing trend with peaks in 2009, 2019, and 2024. ATMPs, introduced in 2005, show pronounced spikes in specific years (2018–2019, 2022), consistent with volatile *R&D* cycles.

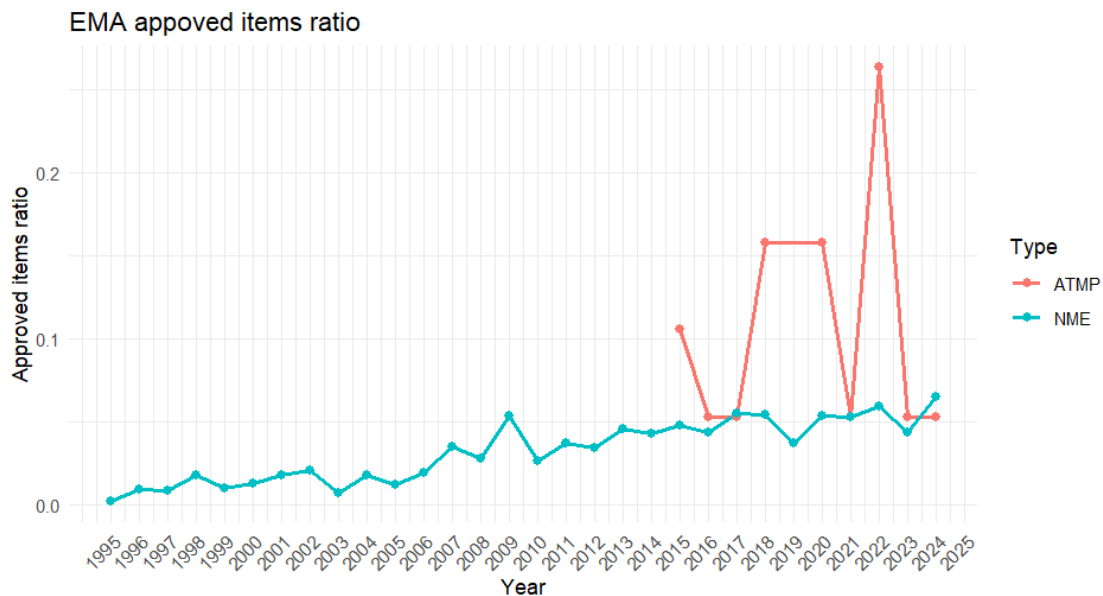


Figure 2: EMA-approved items 1995-2024

United States: LC and CBD M6 with medical innovation versus baseline. For ease of comparison, Figure 3 compares the baseline LC with its adjustment for medical innovation and summarises the main changes in age, period, and innovation.

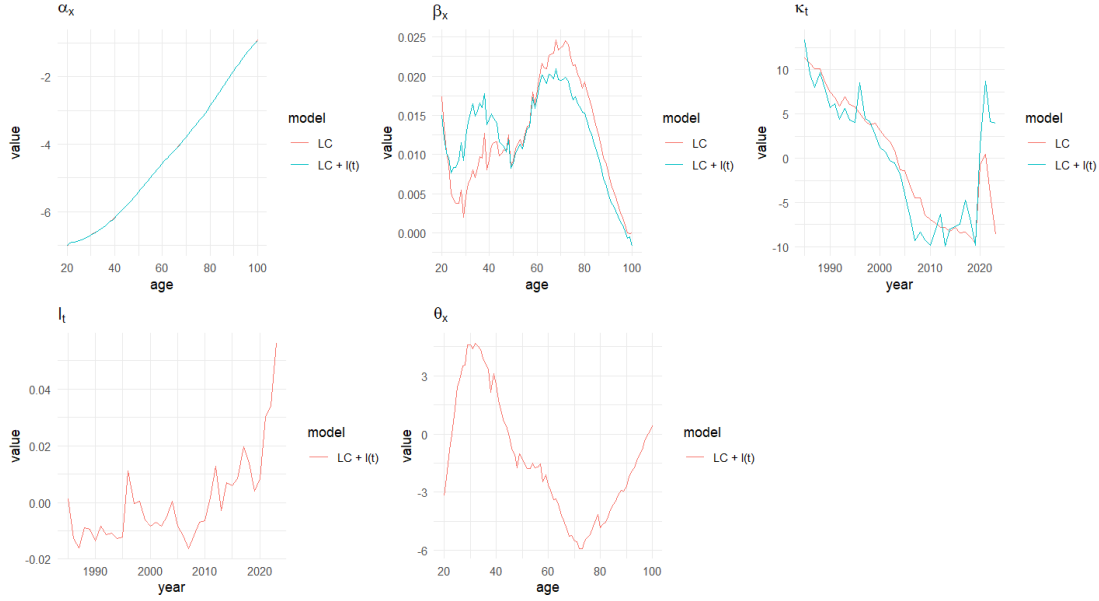


Figure 3: USA LC and extended for $I(t)$ model estimation

The key patterns are as follows. The age effect $\alpha(x)$ is essentially unchanged when adding the innovation indicator. The $\beta(x)$ trend indicates greater volatility associated with medical innovation at younger ages, with relative stability at older ages. The period factor $\kappa(t)$ in the LC model with medical innovation exhibits greater volatility than the baseline, with a marked peak in the late 1990s and early 2000s. In addition, it shows visible oscillations, a slowdown around 2011-2014, and a more substantial COVID-19 impact. The innovation index $I(t)$ increases over time, with growth peaks in the late 1990s-2000s and a pronounced surge in the 2020s. The age-specific parameter $\theta(x)$ shows the most significant sensitivity at ages 20–30, stabilises through ages 40–60, and turns negative at older ages (see Figure 3).

Turning to the CBD M6 specification, Figure 4 compares the baseline model with its innovation-adjusted version and summarises how the inclusion of $I(t)$ reshapes the level, time, and age-specific parameters.

The time-varying level factor $\kappa_1(t)$ better captures the general time pattern once the covariate is included, showing slowdowns and the COVID-19 shock more clearly and yielding lower levels on average. The time-varying age-slope factor $\kappa_2(t)$ measures the sensitivity of age-specific mortality: it shows that divergence at older ages is reduced, with convergence in

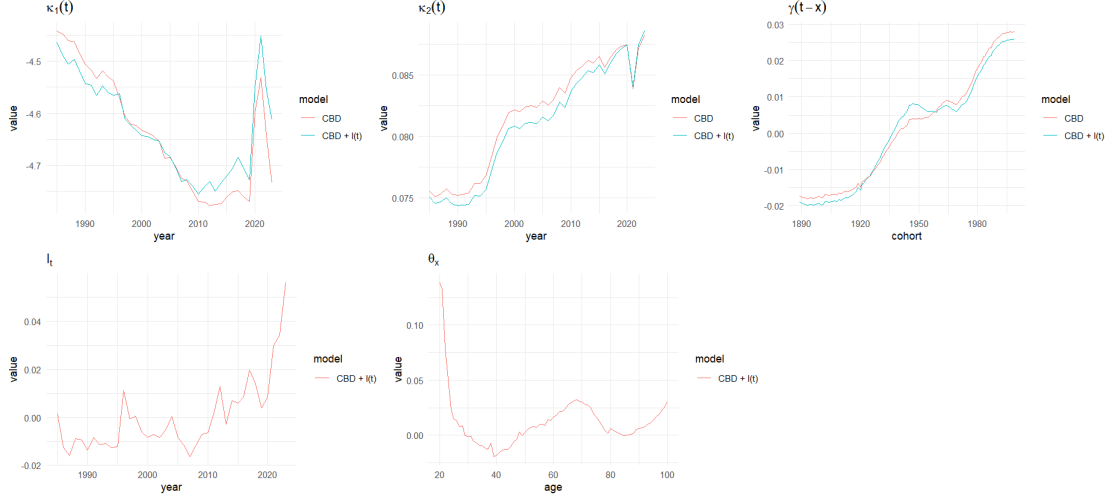


Figure 4: USA CBD M6 and extended for $I(t)$ model estimation

recent years, indicating smaller age disparities. The cohort effect $\gamma(c)$ preserves its overall trend, with a peak around the 1940 cohort and a subsequent slowdown near the 1960 cohort. Consistent with the LC evidence, $I(t)$ follows an increasing, approximately convex path, reflecting the rise of advanced therapies. The parameter $\theta(x)$ is largest at ages 20–30, declines around age 40, and increases again through mid-to-late adulthood, about 40–70, and drops off at the extremes (see Figure 4).

France: LC and CBD M6 with medical innovation versus baseline. Refer to Figure 5 for the LC specification.

With the extension to the medical innovation, the age profile $\alpha(x)$ is essentially unchanged, with the curve that almost perfectly overlaps the baseline. The age-specific sensitivity $\beta(x)$ suggests that pharmaceutical innovation concentrates its effects in middle-aged groups. The period factor κ_t traces a smoother path through the early 2000s, implying lower mortality than that in the baseline; between 2010 and 2014, however, the extended model displays larger fluctuations, whereas the baseline flattens. During the COVID-19 years, the LC extended model registers a more pronounced worsening. For France, the innovation index, $I(t)$, has risen over time and exhibited greater volatility in recent years, consistent with the diffusion of advanced therapies. The age-specific parameter $\theta(x)$ is negative at all ages, showing its

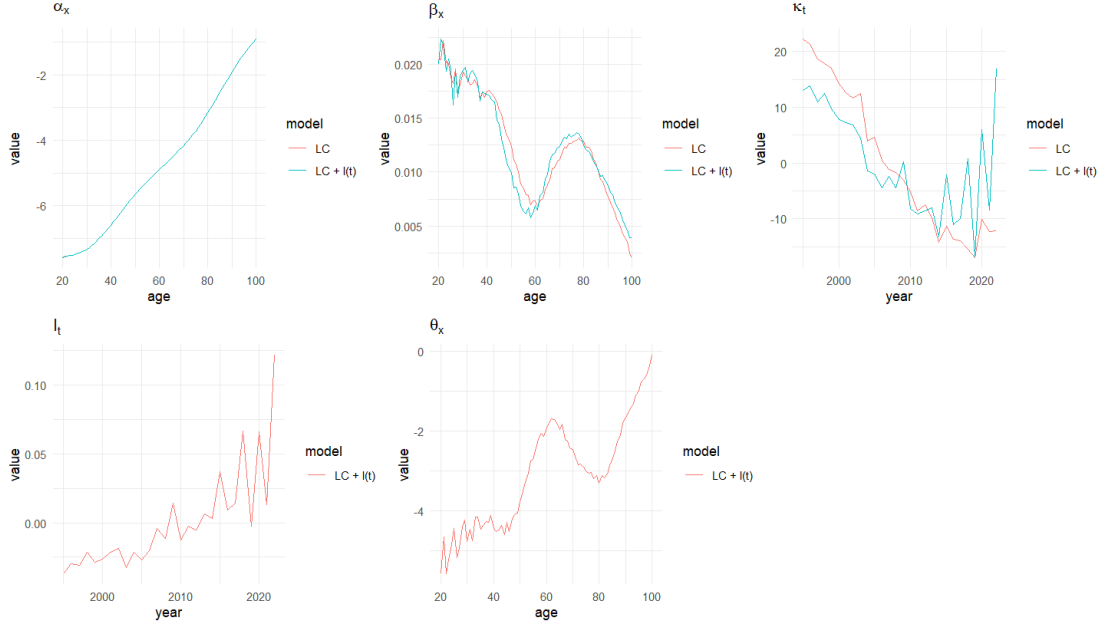


Figure 5: France LC and extended for $I(t)$ model estimation

most substantial impact persists but attenuates at the oldest ages, reaching zero.

For the CBD M6 model, see Figure 6, the level factor $\kappa_1(t)$ shows a flatter evolution from the 1980s to 2000 and, with the covariate included, settles at lower values on average; the extended model is also more volatile and captures slowdowns that the baseline misses.

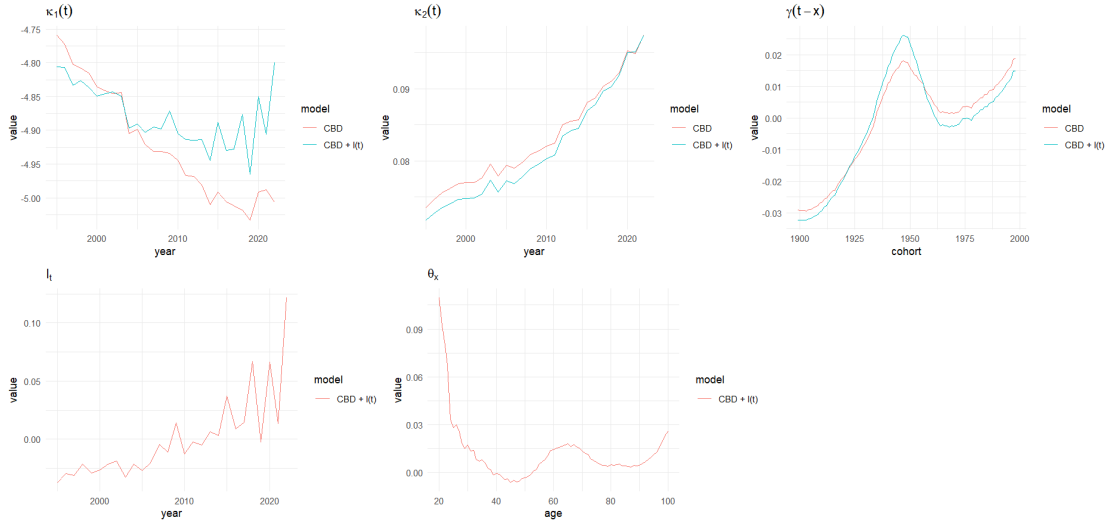


Figure 6: France CBD M6 and extended for $I(t)$ model estimation

The time-varying age-slope factor $\kappa_2(t)$, which measures the sensitivity of age-specific

differences, rises over time but, with the covariate, displays less initial divergence at older ages and a subsequent tendency toward convergence, pointing to reduced age disparities. The cohort effect $\gamma(c)$ maintains its overall profile, with a more pronounced peak around the 1950 cohort, a decline to roughly 1970, and a renewed increase thereafter. The innovation index $I(t)$ trends upward and becomes more volatile after 2010, in line with the arrival of advanced therapies. The parameter $\theta(x)$ is strongest at ages 20–30, falls toward zero near age 40, increases again from 40 to 70 with a peak around age 65, and then diminishes, with a slight uptick at the extremes.

Italy: LC and CBD M6 with medical innovation versus baseline. To assess the role of medical innovation in Italy, Figures 7 and 8 compare the baseline specifications with their innovation extensions and summarise the main shifts in age, period, and cohort components.

For the LC model, see Figure 7, the age profile $\alpha(x)$ is unchanged, with near-identical curves.

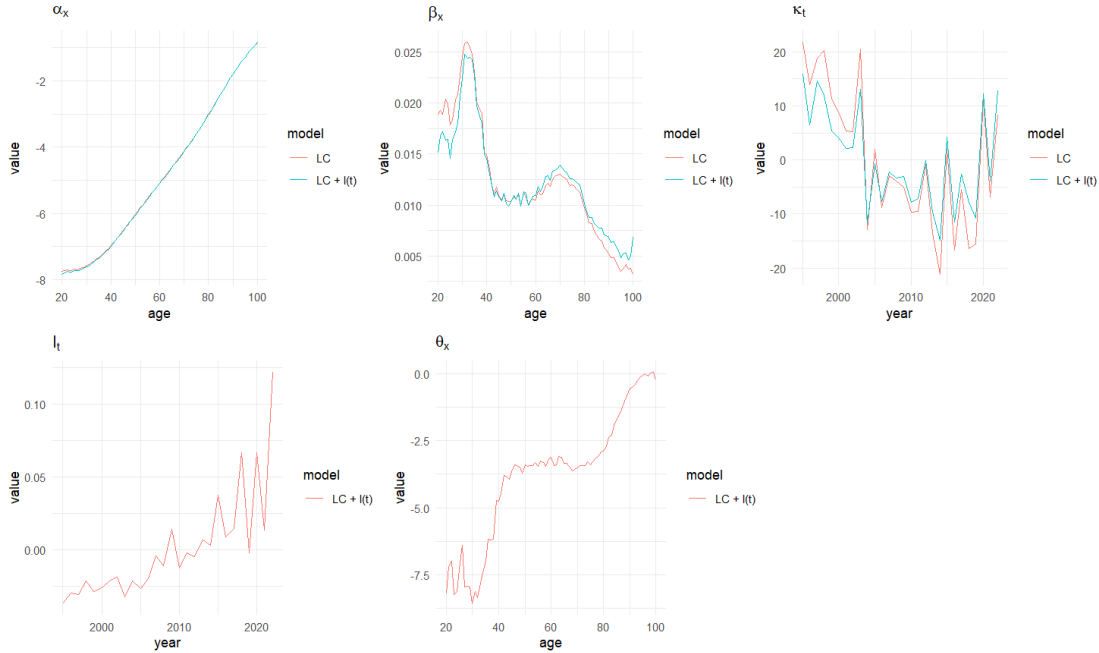


Figure 7: Italy LC and extended for I(t) model estimation

The age-specific parameter $\beta(x)$ exhibits an inverted bell shape, suggesting that the

innovation covariate does not materially alter the age sensitivity. The period factor κ_t remains volatile, with pronounced fluctuations during the COVID-19 years and slightly higher swings under the extended LC model. The innovation index $I(t)$ trends upward with recent surges, reflecting the irregular pace of advanced-therapy adoption. The age-specific sensitivity $\theta(x)$ is negative across ages, indicating that, in Italy, pharmaceutical innovation is associated with a reduction in mortality levels by age.

For the CBD M6 specification, refer to Figure (8).

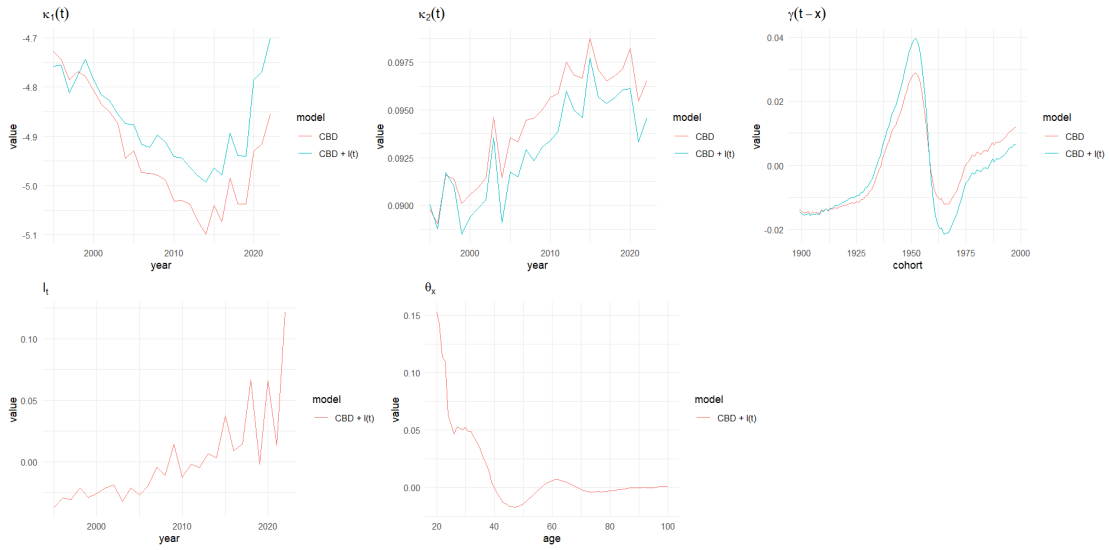


Figure 8: Italy CBD M6 and extended for $I(t)$ model estimation

The level factor $\kappa_1(t)$ points to higher mortality levels and a slower post-2011 decline once the covariate is included. The factor $\kappa_2(t)$ indicates lower age sensitivity and narrower differences across age groups. The cohort effect $\gamma(c)$ preserves its overall shape, with a more pronounced peak for the 1950 cohort and signs that post-1960 cohorts benefit from innovation. The innovation indicator $I(t)$ follows an increasing, approximately quadratic path, with greater volatility in recent years in line with advanced therapies. The sensitivity parameter $\theta(x)$ declines through about age 40, reaches a minimum near age 50, rises again between 50 and 60, then stabilises beyond age 75, with the strongest impact concentrated in the over 50 range.

Implications for Mortality Projections. Finally, we compare projection mortality profiles from LC and CBD-M6 models, with and without the innovation extension for indicator $I(t)$, to assess fit, patterns at different ages, and overall plausibility. In general, across the considered countries, the LC model tends to be more flexible but also more sensitive to noise at extreme ages. Extending LC with $I(t)$ typically improves smoothness and credibility. The CBD M6 model produces stable, nearly linear paths in log-mortality that are well suited to long-term projections: adding $I(t)$ improves realism without sacrificing robustness.

For the United States, see corresponding Figure 9, both the LC and the LC extended model yield smooth projection paths and track observed dynamics well.

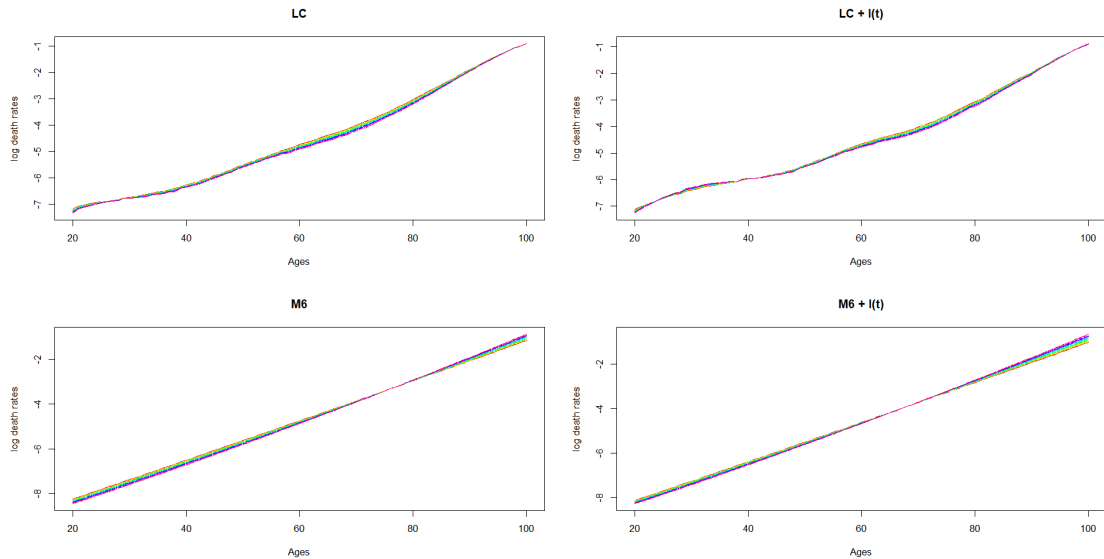


Figure 9: USA mortality rates projections

The CBD M6 model and its extension to medical innovation produce highly linear trends in log-mortality; they are robust but somewhat less flexible around mid-ages.

See the corresponding Figure 10 for France. The LC model application shows greater variability at ages 20–40, whereas the extended LC reduces variance and smooths the curves, improving fit and interpretability.

The CBD M6 specification and its extension remain stable and close to linear, but are

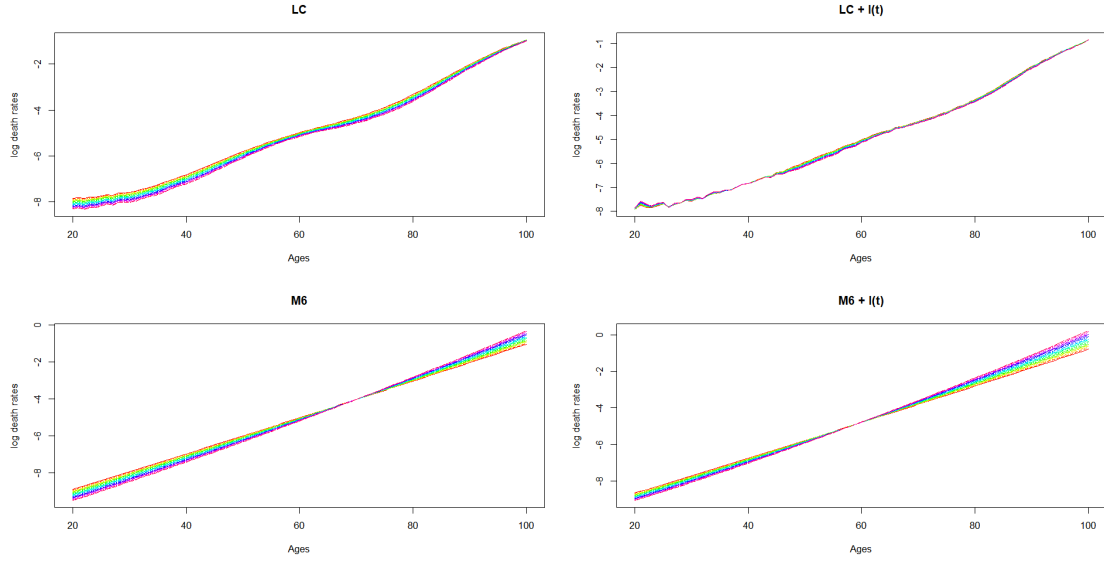


Figure 10: France mortality rates projections

less adaptive to local irregularities.

For Italy, see the corresponding figure 11, the LC exhibits a visible bump at ages 20–40, plausibly reflecting noise or measurement issues.

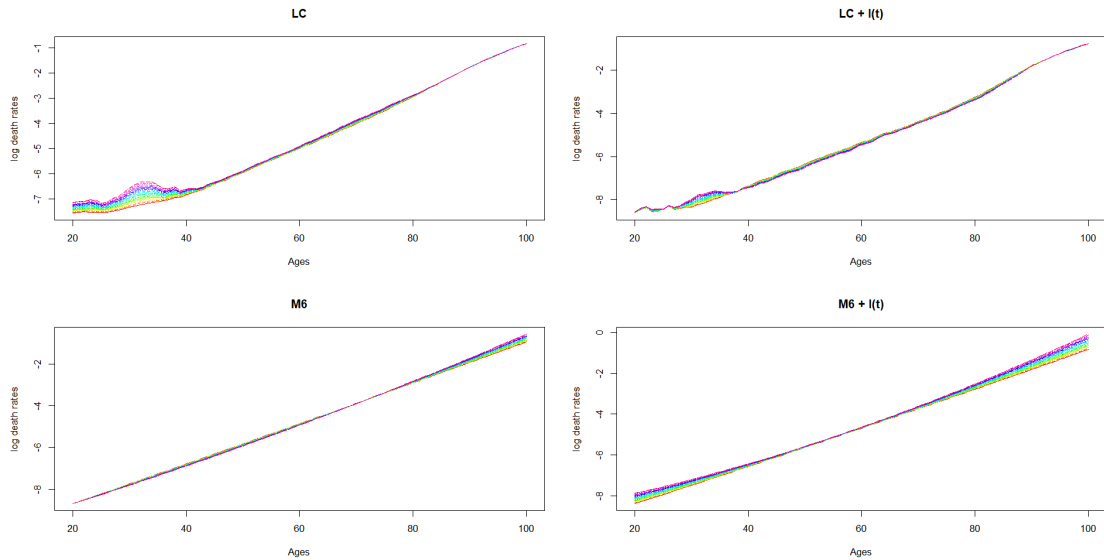


Figure 11: Italy mortality rates projections

The LC extended model for medical innovation attenuates these irregularities, yielding more consistent projections. Applying the CBD M6 and its extension delivers linear, robust

paths but does not resolve low-age irregularities.

5 Conclusion

Medical innovation is a quantitatively relevant driver of mortality dynamics. Embedding an innovation covariate in LC/CBD M6 improves fit and interpretability, with economically meaningful implications for longevity risk management.

In our evidence for the United States, France, and Italy, extending baseline models with an innovation indicator $I(t)$ (constructed from FDA/EMA approvals), systematically sharpens the period fit, capturing slowdowns and COVID-19 amplifications more clearly, stabilising age profiles where LC is most noisy (at young and adult ages), while preserving the baseline age pattern. In addition, the introduction of the age-specific sensitivity $\theta(x)$ implies the evenness of concentrating effects where clinical advances plausibly act more (mid-to-late adulthood), tapering toward the extremes. In the projections, the extended models produce smoother and more credible trends for log-mortality.

From a risk and insurance perspective, the better-identified dynamics, including innovation-aware scenarios, translate into more reliable best-estimate improvements and a narrower model risk for annuity pricing and reserving. They also support more transparent communication of uncertainty by making explicit some links related to therapeutic approvals and new drug diffusion, through which longevity risk evolves.

From a capital management standpoint, the proposed vitagion-augmented models can improve the design and pricing of longevity-linked securities—such as longevity swaps, q-forwards, and survivor bonds—by incorporating prospective medical innovation into expected mortality improvements. This innovation-aware structure can also contribute to more stable Solvency II capital modelling: by explicitly linking future mortality improvements to observable indicators (e.g., FDA/EMA approvals), insurers and pension funds can generate more transparent, evidence-based scenarios for longevity stress testing, ultimately leading

to narrower confidence intervals for the Best Estimate Liability and more reliable Solvency Capital Requirements (SCR).

Our framework suggests several natural extensions. First, quantify how innovation affects best-estimate longevity improvements and annuity pricing. Second, capital impacts under Solvency II should be evaluated when considering the innovation relationship.

References

- Cairns, A. J., Blake, D., and Dowd, K. (2006a). Pricing death: Frameworks for the valuation and securitization of mortality risk. *ASTIN Bulletin: The Journal of the IAA*, 36(1):79–120.
- Cairns, A. J., Blake, D., and Dowd, K. (2006b). A two-factor model for stochastic mortality with parameter uncertainty: theory and calibration. *Journal of Risk and Insurance*, 73(4):687–718.
- Cairns, A. J., Blake, D., Dowd, K., Coughlan, G. D., Epstein, D., Ong, A., and Balevich, I. (2009). A quantitative comparison of stochastic mortality models using data from england and wales and the united states. *North American Actuarial Journal*, 13(1):1–35.
- Carannante, M., D’Amato, V., and Di Palo, C. (2024). Prolonging life by vitagions: modelling of mortality improvement shocks. *Submitted*.
- European Medicines Agency (accessed 2025). European public assessment reports (epar) – download medicine data. <https://www.ema.europa.eu/en/medicines/download-medicine-data>.
- Haberman, S. and Renshaw, A. (2011). A comparative study of parametric mortality projection models. *Insurance: Mathematics and Economics*, 48(1):35–55.
- Human Mortality Database (accessed 2025). Human mortality database. <https://www.mortality.org/>.
- Hunt, A. and Blake, D. (2014). A general procedure for constructing mortality models. *North American Actuarial Journal*, 18(1):116–138.
- Lee, R. D. and Carter, L. R. (1992). Modeling and forecasting u.s. mortality. *Journal of the American Statistical Association*, 87(419):659–671.
- Niu, G. and Melenberg, B. (2014). Trends in mortality decrease and economic growth. *Demography*, 51(5):1755–1773.

- Pitacco, E. (2009). *Modelling longevity dynamics for pensions and annuity business*. Oxford University Press.
- U.S. Food and Drug Administration (accessed 2025a). Approved cellular and gene therapy products. <https://www.fda.gov/vaccines-blood-biologics/cellular-gene-therapy-products/approved-cellular-and-gene-therapy-products>.
- U.S. Food and Drug Administration (accessed 2025b). Compilation of cder nme and new biologic approvals. <https://www.fda.gov/drugs/drug-approvals-and-databases/compilation-cder-new-molecular-entity-nme-drug-and-new-biologic-approvals>.
- U.S. Food and Drug Administration (accessed 2025c). Purple book database of licensed biological products. <https://purplebooksearch.fda.gov/>.
- Woo, G. (2014). Prospective stochastic longevity modelling. *Presented at the Actuarial Society of South Africa*.